

Localized chaos in rotating and charged AdS black holes and their ultraspinning version

Hadyan Luthfan Prihadi,^{1,2,*} Freddy Permana Zen,^{1,2,†} Donny Dwiputra,^{3,‡} and Seramika Ariwahjoedi^{3,4,§}

¹*Theoretical High Energy Physics Group, Department of Physics, FMIPA,
Institut Teknologi Bandung, Jl. Ganesha 10 Bandung, Indonesia.*

²*Indonesia Center for Theoretical and Mathematical Physics (ICTMP),
Institut Teknologi Bandung, Jl. Ganesha 10 Bandung, 40132, Indonesia.*

³*Asia Pacific Center for Theoretical Physics, Pohang University of
Science and Technology, Pohang 37673, Gyeongsangbuk-do, South Korea.*

⁴*Research Center for Quantum Physics, National Research and Innovation Agency (BRIN), South Tangerang 15314, Indonesia.*

(Dated: February 1, 2024)

The butterfly velocity and the Lyapunov exponent of four-dimensional rotating charged asymptotically AdS black holes are calculated to probe chaos using localized rotating and charged shock waves. The localized shocks also generate butterfly velocities which quickly vanish when we approach extremality, indicating no entanglement spread near extremality. One of the butterfly velocity modes is well bounded by both the speed of light and the Schwarzschild-AdS result, while the other may become superluminal. Aside from the logarithmic behavior of the scrambling time which indicates chaos, the Lyapunov exponent is also positive and bounded by $\kappa = 2\pi T_H/(1 - \mu\mathcal{L})$. The Kerr-NUT-AdS and Kerr-Sen-AdS solutions and their ultraspinning versions are used as examples to attain a better understanding of the chaotic phenomena in rotating black holes, especially the ones with extra conserved charges.

I. INTRODUCTION

The study of chaotic behavior of some quantum field theories (especially conformal field theories/CFT) which are conjectured to be dual to black holes has been an interesting and important topic since Shenker and Stanford [1] calculated the scrambling time and the Lyapunov exponent of a BTZ black hole. The Lyapunov exponent of a chaotic system was then found to be bounded from above by its temperature, or surface gravity in the black hole language [2]. Saturation of the upper bound is then suggested to be the sufficient condition of a theory with an Einstein gravity dual. The holographic description [3–7] of chaotic behavior of various black hole spacetimes have been extensively studied [1, 8–22] until very recently. Other than using the holographic principle, chaos in black holes can also be studied using other methods such as the geodesic analysis [23–28]. This work extends the holographic description of chaos in more general rotating and charged Kerr-AdS black holes in four dimensions due to localized perturbations.

An eternal black hole in Anti-de Sitter (AdS) background is suggested to have a CFT dual description described by an entangled thermofield double (TFD) state [29]. This is an alternative description to the near-horizon microscopic description of a black hole via the Kerr/CFT correspondence [30–36]. The chaotic behavior of a black hole is studied by disrupting the entanglement pattern of the TFD state by an operator in the far

past. In the gravity description, the operator is viewed as a gravitational shock wave sent from the past traveling very close to the speed of light near the horizon. Although the shock wave initially has a $\mathcal{O}(\hbar)$ energy, it is then highly blueshifted and becomes of order one before entering the black hole. This process can be described by the shock wave geometry or the Dray-'t Hooft solution. The signature of chaos appears when the four-point out-of-time-ordered correlator (OTOC) approaches zero exponentially and vanishes at time scale τ_* , which is defined to be the scrambling time [1]. For a system with scrambling time proportional to the logarithmic of the system's entropy, the system is said to be a fast scrambler, and black holes are conjectured to be the fastest scrambler in nature [37]. In the holographic description, the OTOC is calculated using the holographic mutual information with the Ryu-Takayanagi [4, 5] and the Hartman-Maldacena [7] surfaces. The OTOC is related to the shock wave profile that enters the black hole [1, 9].

By perturbing the TFD state using local operators, we can also extract information about the effective "light cone" in which the OTOC can only vanish inside it [9]. Such a speed of propagation is defined as the butterfly velocity v_B . For a static black hole in AdS, the butterfly velocity solely depends on the spacetime dimension in the large black hole limit [1, 9].

More general black holes in AdS should also indicate chaos in their boundary theories, including the one with rotation and charges. The uncharged cases were first studied using holography for the Kerr-AdS black hole in 4 and 5 spacetime dimensions [19, 20] and has recently been extended to the Kerr-Sen-AdS₄ black hole as the solution to the Einstein-Maxwell dilaton-axion (EMDA) theory with electromagnetic, dilaton, and axion charges [22]. However, the properties of chaos for more general

* hadyanluthfan@itb.ac.id

† fpzen@fi.itb.ac.id

‡ donny.dwiputra@gmail.com

§ sera001@brin.go.id

Kerr-AdS black holes due to rotating and charged shock waves are still incomplete, especially important information about how local entanglement disruption spread throughout the spacetime is still lacking. The use of rotating (and charged) shock waves might also give us interesting result since it is known that rotating shock waves give a new bound for the Lyapunov exponent [18, 19, 22]. We also consider the ultraspinning limit $a \rightarrow l$, where a is the rotation parameter of the black hole and l is the AdS radius, of the Kerr-AdS black hole solutions. This limit is unique to the rotating AdS black holes and it is interesting to study since the solution will be different compared to the standard Kerr-AdS black hole and not just simply obtained by taking the $a \rightarrow l$ limit of the standard Kerr-AdS black hole solutions.

The study of the chaotic properties of more general rotating black holes is important to further understand the dual CFT theory and gives us insights into understanding the quantum aspects of gravity, which is previously studied using string theory and loop quantum gravity [38, 39], even more.

In this work, we consider more general Kerr-AdS black hole families and calculate their chaotic properties such as the butterfly velocity and the Lyapunov exponent. We find that the butterfly velocity of the rotating black hole in AdS is highly influenced by the black hole rotation parameter a and the shock waves angular momentum \mathcal{L} , as well as the black hole charges. We use the Kerr-NUT-AdS and Kerr-Sen-AdS solutions as examples to test the behavior of the butterfly velocity. We then also check whether the Lyapunov exponent of such black holes is bounded by its surface gravity $\kappa = 2\pi T_H / (1 - \mu\mathcal{L})$ where T_H is the Hawking temperature and μ is the angular momentum of the black hole and compare two results between the Kerr-NUT-AdS and the Kerr-Sen-AdS black hole.

The content structure of this work is as follows: In Sec. II, we briefly write the solutions to the Kerr-NUT-AdS and the Kerr-Sen-AdS black holes that serve as the background in calculating the butterfly velocity. In Sec. III, we derive the Kruskal coordinates from the rotating and charged shock waves perspective. In Sec. IV, we calculate the butterfly velocity of the Kerr-AdS black holes from solving the Einstein's equation sourced by both matter and the localized shock waves. This is the main result of this work. In Sec. V, we calculate the butterfly velocities for the ultraspinning cases. We then plot the Lyapunov exponent of both Kerr-NUT-AdS and Kerr-Sen-AdS black holes to make comparison between the two in Sec. VI. We summarize our results in the Conclusions and Discussions session in Sec. VII.

II. THE KERR-ADS BLACK HOLES AND THEIR ULTRASPINNING LIMIT

In this section, we briefly review the metric of the Kerr-AdS black holes that are used in this work as the back-

ground. The first black hole solution is the charged Kerr-NUT-AdS solution [40]. This solution can be obtained from the general Petrov type D solution of the Einstein's equation with vanishing acceleration parameter [41]. The metric in Boyer-Lindquist coordinates is given by [42]

$$ds^2 = -\frac{\Delta}{\Sigma}X^2 + \frac{\Sigma}{\Delta}dr^2 + \frac{\Sigma}{\Delta_\theta}d\theta^2 + \frac{\Delta_\theta \sin^2 \theta}{\Sigma}Y^2, \quad (1)$$

where

$$X = dt + \frac{(2n \cos \theta - a \sin^2 \theta)}{\Xi}d\varphi, \quad (2)$$

$$Y = a dt - \frac{(r^2 + n^2 + a^2)}{\Xi}d\varphi,$$

$$\Delta(r) = \frac{3(a^2 - n^2)n^2 + (a^2 + 6n^2)r^2 + r^4}{l^2} + r^2 + a^2 - 2mr - n^2 + p^2 + q^2, \quad (3)$$

$$\Delta_\theta = 1 - \frac{4an \cos \theta}{l^2} - \frac{a^2 \cos^2 \theta}{l^2}, \quad \Xi = 1 - \frac{a^2}{l^2}, \quad (4)$$

$$\Sigma = r^2 + (n + a \cos \theta)^2.$$

The function $\Delta(r)$ determines the location of the horizon, with the outermost horizon r_+ is the largest solution to $\Delta(r) = 0$. The parameters in the Kerr-NUT-AdS black holes are $\{m, a, p, q, n, l\}$ which describe its mass, rotation, magnetic charge, electric charge, NUT parameter, and the AdS radius respectively.

On the other hand, the Kerr-Sen-AdS black hole solution is obtained from the equation of motion derived from the gauged Einstein-Maxwell dilaton-axion action [43]. The solution to the equation of motion is given by

$$ds^2 = -\frac{\bar{\Delta}}{\bar{\Sigma}}\bar{X}^2 + \frac{\bar{\Sigma}}{\bar{\Delta}}dr^2 + \frac{\bar{\Sigma}}{\bar{\Delta}_\theta}d\theta^2 + \frac{\bar{\Delta}_\theta \sin^2 \theta}{\bar{\Sigma}}\bar{Y}^2, \quad (5)$$

where

$$\bar{X} = dt - \frac{d \sin^2 \theta}{\bar{\Xi}}d\varphi, \quad (6)$$

$$\bar{Y} = a dt - \frac{(r^2 - d^2 - k^2 + a^2)}{\bar{\Xi}}d\varphi,$$

$$\bar{\Delta}(r) = \left(1 + \frac{r^2 - d^2 - k^2}{l^2}\right)(r^2 - d^2 - k^2 + a^2) - 2mr + p^2 + q^2 \quad (7)$$

$$\bar{\Delta}_\theta = 1 - \frac{a^2 \cos^2 \theta}{l^2}, \quad \bar{\Xi} = 1 - \frac{a^2}{l^2}, \quad (8)$$

$$\bar{\Sigma} = r^2 - d^2 - k^2 + a^2 \cos^2 \theta.$$

Again, the function $\bar{\Delta}(r)$ determines the horizon and the Kerr-Sen-AdS black hole is characterized by

$\{m, a, p, q, d, k, l\}$ which describe its mass, rotation, magnetic charge, electric charge, dilaton charge, axion charge, and AdS radius respectively.

The thermodynamics quantities of the Kerr-NUT-AdS and the Kerr-Sen-AdS black hole are given by

$$\begin{aligned} M &= \frac{m}{\Xi}, \quad J = \frac{ma}{\Xi}, \quad Q = \frac{q}{\Xi}, \quad P = \frac{p}{\Xi}, \quad (9) \\ S &= \frac{\pi}{\Xi}(r_+^2 + \Upsilon^2 + a^2), \\ \Omega_\varphi &= \frac{a\Xi}{r_+^2 + \Upsilon^2 + a^2}, \\ T_H &= \frac{\Delta'(r_+)}{r_+^2 + \Upsilon^2 + a^2}, \end{aligned}$$

where the function Υ^2 is defined to make some distinction between the Kerr-NUT-AdS and the Kerr-Sen-AdS black holes and it is given by

$$\Upsilon^2 = \begin{cases} n^2, & \text{Kerr-NUT-AdS} \\ -d^2 - k^2, & \text{Kerr-Sen-AdS} \\ 0, & \text{Kerr-AdS} \end{cases} \quad (10)$$

The thermodynamics functions denotes the black hole's mass M , conserved angular momentum J , conserved electric charge Q , and conserved magnetic charge P . The entropy of the black hole is given by S while Ω_φ and T_H are the horizon's angular velocity and the Hawking temperature respectively.

The ultraspinning black hole solutions can be obtained by redefining the coordinate $\varphi \rightarrow \varphi/\Xi$ and take the $a \rightarrow l$ limit. The important difference between the standard Kerr-AdS black holes and the ultraspinning versions that is used in this work is the horizon's angular velocity. It is now given by

$$\hat{\Omega}_\varphi = \frac{l}{\hat{r}_+^2 + \Upsilon^2 + l^2}, \quad (11)$$

which works for both the Kerr-NUT-AdS and the Kerr-Sen-AdS black holes. The outer horizon \hat{r}_+ is the largest solution to the $a \rightarrow l$ limit of either $\Delta(r) = 0$ or $\bar{\Delta}(r) = 0$, depending on which background is being used. Therefore, \hat{r}_+ varies with the type of the black hole.

III. KRUSKAL COORDINATES FROM ROTATING CHARGED SHOCK WAVES

Perturbation of the entangled CFT dual of a rotating and charged eternal Kerr-AdS black hole corresponds to gravitational shock waves traveling from the boundary to the interior of the black hole. The geometry of the traveling shock waves is represented by the Dray-'t Hooft solution [44, 45]. The shock waves geometry due to rotating

shock waves with angular momentum \mathcal{L} was first studied in [18] for the three-dimensional BTZ black hole and recently extended to the four-dimensional Kerr-AdS [19] and the Kerr-Sen-AdS black hole [22]. In this work, such a shock wave geometry is used to probe the localized entanglement disruption of a Kerr-AdS black hole families. The gravitational shock waves follow an approximately null-like path denoted by ξ_\pm .

A. Metric in the Kruskal Coordinates

The geodesics ξ_\pm of a null rotating shock wave with energy \mathcal{E} and angular momentum \mathcal{L} satisfy [19]

$$\xi_+^2 = 0, \quad \xi_+ \cdot \zeta_t = -\mathcal{E}, \quad \xi_+ \cdot \zeta_\varphi = \mathcal{L}, \quad \xi_+^\mu K_{\mu\nu} \xi_+^\nu = Q, \quad (12)$$

where $\zeta_t = \partial_t - a/l^2 \partial_\varphi$ and $\zeta_\varphi = \partial_\varphi$ are the Killing vectors correspond to time translation and rotational invariant respectively and $K_{\mu\nu}$ is the Killing-Yano tensor with Carter's constant Q . The explicit form of $K_{\mu\nu}$ and Q is not important and we can solve the geodesics by imposing the boundary condition $\xi^\theta = 0$ at the equator $\theta = \pi/2$. From axisymmetry, we can have other geodesic solutions denoted as ξ_- from reversing the sign of $-\mathcal{E} \rightarrow \mathcal{E}$ and $\mathcal{L} \rightarrow -\mathcal{L}$.

The geodesics are then used to write the Kruskal-like coordinates for equatorial rotating shock waves in the Kerr-AdS background, which is given by

$$\xi_+ \cdot dx = dr_* - d\tau - \xi_\theta d\theta \equiv du, \quad (13)$$

$$\xi_- \cdot dx = dr_* + d\tau + \xi_\theta d\theta \equiv dv, \quad (14)$$

where $\tau = (1 - a\mathcal{L}/l^2)t - \mathcal{L}\varphi$. The tortoise-like coordinate r_* is given by

$$r_*(r) = \int \frac{\tilde{f}}{\Delta} dr, \quad (15)$$

where

$$\tilde{f}^2 = -\Delta(\mathcal{L} - a)^2 + (\mathcal{L}a(1 + (r^2 + \Upsilon^2)/l^2) - (r^2 + \Upsilon^2 + a^2))^2, \quad (16)$$

and the theta component of the geodesics is given by

$$\xi_\theta = \frac{\sqrt{-\Xi \cot^2 \theta (l^2(\Xi - \Delta_\theta) + \mathcal{L}^2 \Delta_\theta)}}{\Delta_\theta}. \quad (17)$$

The metric of the Kerr-AdS black hole in this Kruskal-like coordinates can then be written as

$$ds^2 = F(r, \theta) du dv + h(r, \theta) (dz + h_\tau(r, \theta) d\tau)^2 \quad (18)$$

$$+ g(r, \theta) (d\theta + g_\tau(r, \theta) d\tau)^2, \quad (19)$$

where the explicit form of the functions $\{F, h, h_\tau, g, g_\tau\}$ are given by

$$\begin{aligned}
F(r, \theta) &= \frac{\Delta \Sigma}{\tilde{f}^2}, \\
h(r, \theta) &= \eta^2 \frac{(\Delta_\theta \sin^2 \theta (\mathcal{L} a (1 + (r^2 + \Upsilon^2)/l^2) - (r^2 + \Upsilon^2 + a^2))^2 - \Delta (\mathcal{L} \Delta_\theta - a \sin^2 \theta)^2)}{\Sigma (1 - a \mathcal{L}/l^2)^2 \Xi^2}, \\
h_\tau(r, \theta) &= \eta^{-1} \left[\frac{\Xi (a \sin^2 \theta \Delta_\theta (a \mathcal{L} (1 + (r^2 + \Upsilon^2)/l^2) - (r^2 + \Upsilon^2 + a^2)) - \Delta (\mathcal{L} \Delta_\theta - a \sin^2 \theta))}{\Delta_\theta \sin^2 \theta (\mathcal{L} a (1 + (r^2 + \Upsilon^2)/l^2) - (r^2 + \Upsilon^2 + a^2))^2 - \Delta (\mathcal{L} \Delta_\theta - a \sin^2 \theta)^2} + \gamma \right], \\
g(r, \theta) &= \frac{\Sigma (\Delta_\theta \sin^2 \theta (\mathcal{L} a (1 + (r^2 + \Upsilon^2)/l^2) - (r^2 + \Upsilon^2 + a^2))^2 - \Delta (\mathcal{L} \Delta_\theta - a \sin^2 \theta)^2)}{\tilde{f}^2 \Delta_\theta^2 \sin^2 \theta}, \\
g_\tau(t, \theta) &= \frac{\Delta \Delta_\theta \sin^2 \theta \sqrt{-\Xi \cot^2 \theta (l^2 (\Xi - \Delta_\theta) + \Delta_\theta \mathcal{L}^2)}}{\Delta_\theta \sin^2 \theta (\mathcal{L} a (1 + (r^2 + \Upsilon^2)/l^2) - (r^2 + \Upsilon^2 + a^2))^2 - \Delta (\mathcal{L} \Delta_\theta - a \sin^2 \theta)^2}.
\end{aligned} \tag{20}$$

Here, we have performed coordinate transformation $\varphi \rightarrow \eta z + \gamma \tau$ such that $h_\tau(r)$ behaves as $\mathcal{O}(r - r_+)$ near the horizon and recover the black hole horizon area when z is integrated from 0 to 2π , following [19, 22]. In this case, we have $\eta = \frac{1}{1-\mu\mathcal{L}}$ and $\gamma = \frac{\Omega_\varphi}{1-\mu\mathcal{L}}$ with $\mu \equiv \Omega_\varphi + a/l^2$.

The metric in the affine coordinates at r_+ , $U = -e^{\kappa u}$ and $V = e^{\kappa v}$, where $\kappa = \frac{2\pi T_H}{1-\mu\mathcal{L}}$, can be written as

$$\begin{aligned}
ds^2 &= \frac{F}{\kappa^2 UV} dU dV \\
&+ h \left(dz + \frac{h_\tau}{2\kappa UV} (U dV - V dU) - h_\tau \xi_\theta d\theta \right)^2 \\
&+ g \left(d\theta + \frac{g_\tau}{2\kappa UV} (U dV - V dU) - g_\tau \xi_\theta d\theta \right)^2.
\end{aligned} \tag{21}$$

We use this coordinate to generate the Dray-'t Hooft solution due to the rotating and charged shock waves. Later on, we write the functions as $\{F(r), h(r), h_\tau(r), g(r), g_\tau(r)\}$ for the equatorial case with $\theta = \pi/2$.

B. Location of the Asymptotic

Consider again the Kerr-AdS black hole metric in Kruskal coordinates at the equator with $\theta = \pi/2$, which is given by

$$ds^2 = \frac{F}{\kappa^2 UV} dU dV + h(dz + h_\tau d\tau)^2. \tag{22}$$

In this subsection, we would like to derive the asymptotic metric with the existence of the shock waves angular momentum \mathcal{L} . At the asymptotic, the radial value becomes $r \rightarrow r_c \gg 1$. The functions in the metric then becomes

$$\tilde{f}(r_c)^2 \approx r_c^4 \Xi (1 - \mathcal{L}^2/l^2), \tag{23}$$

$$h(r_c) \approx \frac{r_c^2 (1 - \mathcal{L}^2/l^2)}{\Xi (1 - \mu\mathcal{L})^2 (1 - a\mathcal{L}/l^2)^2}, \tag{24}$$

$$h_\tau(r_c) \approx (1 - \mu\mathcal{L}) \left[\frac{(a - \mathcal{L})/l^2}{1 - \mathcal{L}/l^2} + \frac{\Omega_\varphi}{1 - \mu\mathcal{L}} \right], \tag{25}$$

$$F(r_c) \approx \frac{r_c^2/l^2}{\Xi (1 - \mathcal{L}/l^2)}. \tag{26}$$

From this asymptotic limit, the Kerr-AdS black hole metric becomes

$$\begin{aligned}
ds^2 &\approx \frac{r_c^2/l^2}{\Xi (1 - \mathcal{L}/l^2)} \left[-d\tau^2 \right. \\
&\left. + l^2 \left(\frac{(1 - \mathcal{L}^2/l^2)}{(1 - \mu\mathcal{L})(1 - a\mathcal{L}/l^2)} \right)^2 (dz - \omega d\tau)^2 \right].
\end{aligned} \tag{27}$$

The metric inside the square bracket denotes flat space-time in a polar coordinates with radius

$$\bar{r}_c(\mathcal{L}) = l \left(\frac{(1 - \mathcal{L}^2/l^2)}{(1 - \mu\mathcal{L})(1 - a\mathcal{L}/l^2)} \right), \tag{28}$$

and rotating with angular velocity $\omega = h_\tau(r_c)$. The radius of the asymptotic determines $\bar{r}_c(\mathcal{L})$ as the prefactor of the butterfly velocity which will be represented later on in order to represent the velocity as a tangential velocity at the asymptotic instead of an angular velocity. The radius $\bar{r}_c(\mathcal{L})$ depends on the angular velocity of the shock waves \mathcal{L} and reduce to the standard radius in black hole with AdS background $\bar{r}_c(0) = l$ when the angular momentum vanishes.

IV. LOCALIZED DRAY-'T HOOFT SOLUTION AND BUTTERFLY VELOCITIES

A. Einstein's Equation

The shock wave solution can be obtained by using the shift in the V coordinate such that $V \rightarrow V + \alpha f(z, \theta) \Theta(U - U_0)$, where $\Theta(U - U_0)$ denotes the Heaviside step function. The value of the shift is expressed by the parameter $\alpha f(z, \theta)$, which can be a function of τ ,

θ and z . If we choose the perturbations to always stay at the equator, then $\alpha f(z)$ can only be the function of τ and z . After the coordinate shift, the metric becomes

$$ds^2 \rightarrow \tilde{ds}^2 - \left(\frac{F}{\kappa^2 UV} \right) \alpha f(z) \delta(U) dU^2. \quad (29)$$

This solves the Einstein equation with cosmological constant $\Lambda = -\frac{3}{l^2}$ sourced by both matter and shock waves energy-momentum tensor

$$R_{\mu\nu} - \frac{1}{2} R g_{\mu\nu} + \Lambda g_{\mu\nu} = 8\pi G_N (T_{\mu\nu}^{\text{matter}} + T_{\mu\nu}^{\text{shocks}}). \quad (30)$$

The form of $T_{\mu\nu}^{\text{shocks}}$ depends on the shock waves profile. For localized equatorial shock waves along the $U = \text{const.}$ trajectory, the energy-momentum of the shocks can be written as

$$T_{UU}^{\text{shocks}} = \mathbb{B} \alpha \delta(z - z_0) \delta(U) dU^2, \quad (31)$$

where \mathbb{B} is some constant that depends on the energy of the shock waves and we choose point source $\delta(z - z_0)$ to describe the localized shock wave profile. Here we assume that the shock waves always stay along the equator and hence its profile does not depend on θ .

The energy-momentum tensor for the matter fields is given by

$$\begin{aligned} T_{\mu\nu}^{\text{matter}} dx^\mu dx^\nu & \\ = & T_{UU} dU^2 + 2T_{UV} dU dV + T_{VV} dV^2 \\ & + T_{zz} dz^2 + 2T_{Uz} dU dz + 2T_{Vz} dV dz. \end{aligned} \quad (32)$$

For rotating black hole with axial symmetry, there are crossing terms between time coordinate t and the axial coordinate φ . The crossing term is depicted by both Vz and Uz components of the energy-momentum tensor. After the shift in the V -direction, the energy-momentum tensor becomes

$$\begin{aligned} T_{\mu\nu}^{\text{matter}} dx^\mu dx^\nu & \\ = & (T_{UU} - 2T_{UV} \alpha f(z) \delta(U) + T_{VV} \alpha^2 f(z)^2 \delta(U)^2) dU^2 \\ & + (2T_{UV} - 2T_{Vz} \alpha f(z) \delta(U)) dU dV \\ & (2T_{Uz} - 2T_{Vz} \alpha f(z) \delta(U)) dU dz \\ & + T_{zz} dz^2 + 2T_{Vz} dV dz. \end{aligned} \quad (33)$$

The value of α can be obtained by considering the smoothness of the geometry at the horizon and using the first-law of thermodynamics for the rotating AdS black hole. From the calculations performed in [22], we have

$$\alpha = \varepsilon e^{\kappa \tau_0}, \quad (34)$$

where ε depends on the energy of the shock waves. Upon taking the double-scaling limit $\varepsilon \rightarrow 0$ and $e^{\kappa \tau_0} \rightarrow \infty$, the value of α can be of order 1 and becomes significant at late times. But first, in deriving the Einstein's equation,

we treat the function α perturbatively.

In order to obtain the function $f(z)$, we need to solve the Einstein's field equation sourced by both T^{matter} and T^{shocks} in eq. (30). In order to do so, we treat the parameter α as a small parameter by scaling $\alpha \rightarrow \varepsilon \alpha$ and $T^{\text{shocks}} \rightarrow \varepsilon T^{\text{shocks}}$ in which $\varepsilon = 0$ reproduces the unperturbed equation of motion. The Einstein's equation sourced only by T^{matter} is automatically satisfied at $\varepsilon = 0$ and we take the solution to be the Kerr-AdS black hole families.

We then expand the Einstein's equation in the power of ε . The UV component of the Einstein's equation at $\mathcal{O}(\varepsilon)$ and the UU component at $\mathcal{O}(\varepsilon^2)$ are respectively given by

$$\begin{aligned} & \left[\left(\frac{F}{\kappa^2 UV} \right)_{,V} \left(\frac{\kappa^2 UV}{F} \right) \frac{h_{,V}}{2h} + \frac{h_{,V}^2}{2h^2} - \frac{h_{,VV}}{h} \right] \delta(U) f(z) \alpha \\ & = 8\pi G_N T_{VV} \delta(U) f(z) \alpha, \end{aligned} \quad (35)$$

and

$$\begin{aligned} & \left[\left(\frac{F}{\kappa^2 UV} \right)_{,V} \left(\frac{\kappa^2 UV}{F} \right) \frac{h_{,V}}{h} + \frac{h_{,V}^2}{h^2} - \frac{2h_{,VV}}{h} \right] \delta(U)^2 f(z)^2 \alpha^2 \\ & = 8\pi G_N T_{VV} \delta(U)^2 f(z)^2 \alpha^2. \end{aligned} \quad (36)$$

From these two equations, we set [10]

$$\left(\frac{F}{\kappa^2 UV} \right)_{,V} = h_{,V} = h_{,VV} = 0, \quad (37)$$

at the horizon and hence $T_{VV} = 0$ at the horizon. Using those conditions, the Uz component at $\mathcal{O}(\varepsilon)$ and the Vz component at $\mathcal{O}(1)$ of the Einstein's equation are respectively given by

$$\left[\left(\frac{\kappa^2 UV}{F} \right) \left(\frac{h_\tau}{2\kappa UV} \right)_{,V} (6h) - \left(\frac{\kappa^2 UV}{F} \right)^2 \left(\frac{h_\tau}{2\kappa UV} \right) \right] \quad (38)$$

$$\begin{aligned} & \left(\frac{F}{\kappa^2 UV} \right)_{,VV} (2hV) + \left(\frac{\kappa^2 UV}{F} \right) \left(\frac{h_\tau}{2\kappa UV} \right)_{,VV} (2hV) \\ & \times \delta(U) f(z) \alpha = -8\pi G_N T_{Vz} \delta(U) f(z) \alpha, \end{aligned}$$

and

$$\begin{aligned} & - \left(\frac{\kappa^2 UV}{F} \right) \left(\frac{h_\tau}{2\kappa UV} \right)_{,V} (3h) - \left(\frac{\kappa^2 UV}{F} \right) \left(\frac{h_\tau}{2\kappa UV} \right)_{,VV} (39) \\ & \times (hV) = 8\pi G_N T_{Vz}. \end{aligned}$$

The Vz component with $\mathcal{O}(1)$ is automatically satisfied by the equation of motion. Thus, we can insert the value of T_{Vz} into eq. (38). This gives us

$$\left(\frac{h_\tau}{2\kappa UV} \right)_{,V} = \left(\frac{h_\tau}{2\kappa UV} \right)_{,VV} = \left(\frac{F}{\kappa^2 UV} \right)_{,VV} = 0, \quad (40)$$

at the horizon, and hence we also have $T_{Vz} = 0$ at the horizon. The other components of the Einstein's equation with $\mathcal{O}(1)$ are automatically satisfied by the equation of motion. Another important equation at $\mathcal{O}(1)$ is the UV component at $\mathcal{O}(1)$, which is given by

$$\begin{aligned} & -\frac{1}{2l^2} \left(\frac{F}{\kappa^2 UV} \right) + \left(\frac{\kappa^2 UV}{F} \right) \left(\frac{h_\tau}{2\kappa UV} \right)^2 (2h) + \frac{h_{,UV}}{2h} \\ & = 8\pi G_N T_{UV}. \end{aligned} \quad (41)$$

Here, we obtain the value of T_{UV} , which can be inserted into the UU component at $\mathcal{O}(\varepsilon)$. By inserting the T_{UU}^{shocks} from eq. (31) into the UU component of the Einstein's equation at $\mathcal{O}(\varepsilon)$, we have

$$\begin{aligned} & \left(\frac{F}{\kappa^2 UV} \right) \frac{1}{2h} f''(z) \delta(U) - \left(\frac{h_\tau}{\kappa UV} \right) f'(z) \delta(U) \\ & - \frac{h_{,UV}}{h} f(z) \delta(U) = 8\pi G_N \mathbb{B} \delta(z - z_0) \delta(U). \end{aligned} \quad (42)$$

All of the components in the equation are evaluated at the horizon since it is multiplied by $\delta(U)$. The relation between the coordinate r and UV is given by [22]

$$(r - r_+) F'(r_+) = -\mathbb{A} UV, \quad (43)$$

for some dimensionless constant \mathbb{A} . Therefore, we have

$$\left(\frac{F}{\kappa^2 UV} \right) \frac{1}{2h} \Big|_{U=0} = -\frac{\mathbb{A}}{\kappa^2} \frac{1}{2h(r_+)}, \quad (44)$$

$$\left(\frac{h_\tau}{\kappa UV} \right) \Big|_{U=0} = -\frac{\mathbb{A}}{F'(r_+)} \frac{h'_\tau(r_+)}{\kappa}, \quad (45)$$

$$\frac{h_{,UV}}{2h} \Big|_{U=0} = -\frac{\mathbb{A}}{F'(r_+)} \frac{h'(r_+)}{2h(r_+)}. \quad (46)$$

The constant \mathbb{A} can be put into the right hand side of eq. (42). The equation of motion for $f(z)$ reduces to the well-known result such as the one found in [10] if we take the non-rotating and uncharged case.

B. Localized Shocks and Butterfly Velocities

From the previous derivations, the equation for $f(z)$ can be written as

$$(A \partial_z^2 - B \partial_z - C) f(z) = \# \delta(z - z_0), \quad (47)$$

where $\#$ denotes some constant that depends on the energy of the shock waves and

$$A = \frac{1}{2\kappa^2 h(r_+)}, \quad B = \frac{h'_\tau(r_+)}{\kappa F'(r_+)}, \quad C = \frac{h'(r_+)}{2h(r_+)} \frac{1}{F'(r_+)}. \quad (48)$$

Note that z is a periodic function with periodicity 2π . The solution to the differential equation of $f(z)$ reads

$$\begin{aligned} \alpha f(z) & \sim \frac{2\pi}{w_+ - w_-} \frac{e^{\kappa\tau_0 - |w_+|(z-z_0)}}{1 - e^{2\pi w_+}} \\ & + \frac{2\pi}{w_+ - w_-} \frac{e^{\kappa\tau_0 + |w_-|(z-z_0)}}{e^{2\pi w_-} - 1}, \end{aligned} \quad (49)$$

up to some constant that depends on \mathbb{B} and the other parameters of the black hole, with

$$w_\pm \equiv \frac{B}{2A} \pm \sqrt{\left(\frac{B}{2A} \right)^2 + \frac{C}{A}}. \quad (50)$$

The result shows us that the perturbations spread throughout the entire region with velocity (called the butterfly velocity) given by

$$v_B^\pm = \frac{l(1 - \mathcal{L}^2/l^2)}{(1 - \mu\mathcal{L})(1 - a\mathcal{L}/l^2)} \frac{\kappa}{|w_\pm|}. \quad (51)$$

The prefactor comes from the asymptotic radius of the Kerr-AdS metric in a rotating shock wave frame which is given by eq. (28). For the non-rotating, uncharged black hole and static shock wave limit $a, q, p, n, \mathcal{L} \rightarrow 0$, the butterfly velocities reduce to the well-known universal result $v_{B0} = \sqrt{3}/2$ for a static black hole in 4 dimension [1], in large black hole limit $r_+/l \gg 1$.

In contrast to the static case, for the rotating Kerr-AdS black hole, there is the B term which will vanish in the static and neutral case. This term also causes the absolute value of positive v_B^+ and negative v_B^- butterfly velocities to differ, thus breaking the symmetry of the butterfly velocities for static black holes. In the static case, the left- and right-moving butterfly velocities should only differ by a negative sign while in the rotating case, they are influenced by the direction of the rotation of the black hole and the shock waves. Such a term also appear in various calculations involving the rotating BTZ black hole [18, 46]. For $\mathcal{L} = 0$ and vanishing charges, the result agrees with the perturbative result found in [17], while in this work, we obtain the non-perturbative result of the butterfly velocity.

For rotating cases, there are two kinds of butterfly velocities traveling in the opposite direction. Furthermore, the two velocities get shifted due to the rotation of the black holes such that $v_B^+ \neq -v_B^-$. To see the behavior of v_B^\pm for various black hole parameter values, we plot the result as a function of the ratio $\mathfrak{r} \equiv \frac{r_-}{r_+}$ in Fig. 1. In this case, we scale the angular velocity of the shock waves as $\mathcal{L} = sr/\mu$ and vary s . We see that at some values of black hole parameters, the negative modes of the butterfly velocities v_B^- become greater than the speed of light $c = 1$ while the positive mode v_B^+ is well bounded by both c and the Schwarzschild-AdS limit $v_{B0} = \sqrt{3}/2$. This $v_B^- > c$ phenomena also appear in the BTZ case where one of the butterfly velocity becomes greater than the speed of light [14].

In the extremal limit $\tau \rightarrow 1$, the butterfly velocities quickly approach zero, indicating that chaos does not spread in the rotating extremal black holes in AdS. Furthermore, increasing the shock waves' angular momentum \mathcal{L} opts to increase the butterfly velocity. The calculation of the butterfly velocity done in [17] has some drawbacks since it cannot investigate how localized perturbation spreads in the extremal limit.

Some other remarks can be made from the result of the butterfly velocities. Both Kerr-Sen-AdS and Kerr-NUT-AdS give us similar behaviors. In the $\tau \rightarrow 0$ limit, v_B^- and v_B^+ does not coincide since this limit does not necessarily correspond to $\frac{B}{2A} \rightarrow 0$. This is because we are working with both charged and rotating black holes. Although we consider the $a = 0$ case, v_B^- and v_B^+ also do not coincide again due to the existence of the electromagnetic charges. Only when $a, q, p, \mathcal{L} \rightarrow 0$, the butterfly velocities v_B^\pm differ solely by a negative sign.

It is also important to notice that the butterfly velocity v_B^\pm in $s = 1$ case blows up in the extremal limit due to the factor $(1 - \mu\mathcal{L})^{-1}$ in the formulation of the butterfly velocity, which diverges as we approach extremality. This might indicate that such a limit might not be physical in this frame of reference although, as we will see in section VI, the Lyapunov exponent has some finite and nonzero value at this limit. This observation will be important to understand chaos at extremality.

V. CASE FOR THE ULTRASPINNING BLACK HOLES

In this section, we would like to calculate the butterfly velocity of the ultraspinning counterparts of both Kerr-NUT-AdS and Kerr-Sen-AdS black holes. The ultraspinning limit is obtained by first redefining the coordinate $\varphi \rightarrow \varphi/\Xi$ and then taking the limit $a \rightarrow l$ [43]. Following previous derivation of the Kruskal-like metric (see also [22]), the solution for the ultraspinning black hole at $\theta = \pi/2$ is given by

$$ds^2 = \frac{\hat{F}}{\hat{\kappa}^2 \hat{U} \hat{V}} d\hat{U} d\hat{V} + \hat{h}(r) \left(d\hat{z} + \frac{\hat{h}_{\hat{\tau}}(r)}{2\hat{\kappa} \hat{U} \hat{V}} (\hat{U} d\hat{V} - \hat{V} d\hat{U}) \right)^2. \quad (52)$$

The hatted functions are all given by [22]

$$\hat{F}(r) = \frac{\hat{\Delta}(r^2 + \Upsilon^2)}{\hat{f}^2}, \quad (53)$$

$$\hat{h}(r) = \hat{\eta}^2 \frac{\hat{f}^2}{r^2 + \Upsilon^2}, \quad (54)$$

$$\hat{h}_{\hat{\tau}}(r) = \hat{\eta}^{-1} \left[\frac{-\hat{\Delta}(\mathcal{L} - l) + l(\mathcal{L}l - (r^2 + \Upsilon^2 + l^2))}{\hat{f}^2} + \hat{\gamma} \right], \quad (55)$$

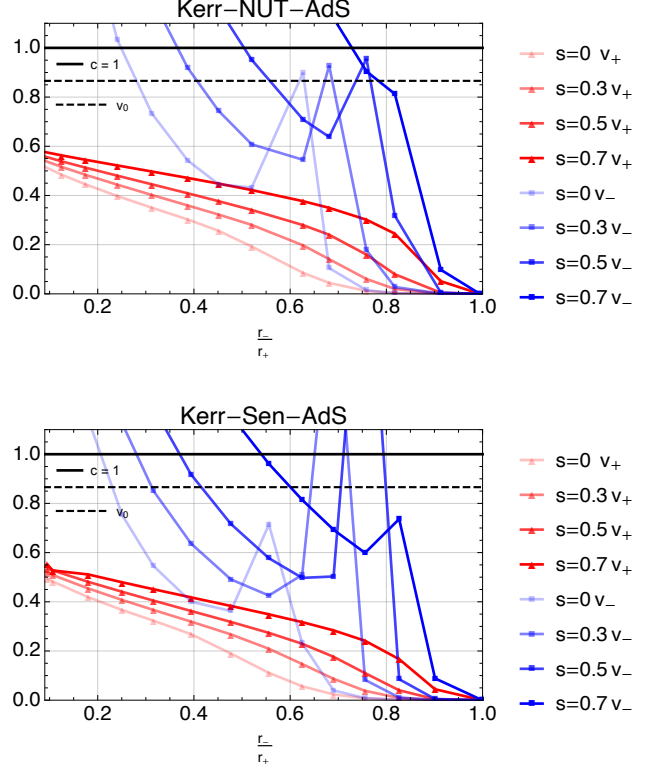


FIG. 1. Plot for the butterfly velocities v_B^\pm for various angular momentum \mathcal{L} which is scaled as $\mathcal{L} = sr/\mu$. We plot for $s = \{0, 0.3, 0.5, 0.7\}$ from $s = 0$ which is depicted by the line with lowest opacity up to $s = 0.7$ which is the one with solid line. Blue lines represent v_B^- while red lines represent v_B^+ . The solid black line represent the speed of light $c = 1$ while the dashed black line represent the Schwarzschild butterfly velocity bound $v_{B0} = \sqrt{3}/2$.

with

$$\hat{f}^2 = -\hat{\Delta}(\mathcal{L} - l)^2 + (\mathcal{L}l - (r^2 + \Upsilon^2 + l^2))^2, \quad (56)$$

$$\hat{\eta} = \frac{1}{1 - \hat{\Omega}_\varphi \mathcal{L}}, \quad \hat{\gamma} = \frac{\hat{\Omega}_\varphi}{1 - \hat{\Omega}_\varphi \mathcal{L}}.$$

The location of the asymptotic for the ultraspinning case is also modified and it is not simply obtained by taking the limit $a \rightarrow l$ of the radius $\bar{r}_c(\mathcal{L})$ in eq. (28). The asymptotic values of the hatted functions obtained by taking $r \rightarrow r_c \gg 1$ are given by

$$\hat{f}(r_c)^2 \approx \frac{r_c^4 \mathcal{L}}{l} \left(2 - \frac{\mathcal{L}}{l} \right), \quad (57)$$

$$\hat{h}(r_c) \approx \frac{r_c^2 \frac{\mathcal{L}}{l} (2 - \frac{\mathcal{L}}{l})}{(1 - \hat{\Omega}_\varphi \mathcal{L})^2},$$

$$\hat{h}_{\hat{\tau}}(r_c) \approx (1 - \hat{\Omega}_\varphi \mathcal{L}) \left[-\frac{l^2 (1 - \mathcal{L}/l)}{\mathcal{L} (2 - \mathcal{L}/l)} + \frac{\hat{\Omega}_\varphi}{1 - \hat{\Omega}_\varphi \mathcal{L}} \right], \quad (58)$$

$$\hat{F}(r_c) \approx \frac{r_c^2 l / \mathcal{L}}{(2 - \mathcal{L}/l)}.$$

From here, the metric of the ultraspinning Kerr-AdS black hole in the asymptotic analogous to eq. (27) is given by

$$ds^2 = \frac{r_c^2 l / \mathcal{L}}{(2 - \mathcal{L}/l)} \left[d\hat{\tau}^2 + \left(\frac{\mathcal{L}/l(2 - \mathcal{L}/l)}{(1 - \hat{\Omega}_\varphi \mathcal{L})} \right)^2 (d\hat{z} - \hat{\omega} d\hat{\tau})^2 \right]. \quad (59)$$

Therefore, for the ultraspinning case, the asymptotic radius $\hat{r}_c(\mathcal{L})$ is given by

$$\hat{r}_c(\mathcal{L}) = \frac{\mathcal{L}/l(2 - \mathcal{L}/l)}{(1 - \hat{\Omega}_\varphi \mathcal{L})}. \quad (60)$$

The result $\hat{r}_c(\mathcal{L})$ differs from the asymptotic radius of the standard Kerr-AdS black hole $\bar{r}_c(\mathcal{L})$ in eq. (28). The asymptotic radius $\hat{r}_c(\mathcal{L})$ is not simply obtained by taking the $a \rightarrow l$ limit of $\bar{r}_c(\mathcal{L})$. Furthermore, the radius $\hat{r}_c(\mathcal{L})$ vanishes when $\mathcal{L} \rightarrow 0$, while the radius $\bar{r}_c(\mathcal{L})$ survives the limit. This result will determine the behavior of the butterfly velocity for the ultraspinning black holes.

The equation of motion for the shift function $\hat{f}(z)$ in the ultraspinning case also follows from the standard Kerr-AdS black holes, but with all functions replaced by the hatted functions. This is because the metric of the ultraspinning black holes in the Kruskal coordinates is in the same form with the standard Kerr-AdS counterpart (see eq. (21) for $\theta = \pi/2$ and eq. (52)). Therefore, the butterfly velocity for the ultraspinning case is given by

$$\hat{v}_B^\pm = \frac{\mathcal{L}/l(2 - \mathcal{L}/l)}{(1 - \hat{\Omega}_\varphi \mathcal{L})} \frac{\hat{\kappa}}{|\hat{w}_\pm|}, \quad (61)$$

where now \hat{w}_\pm is given by

$$\hat{w}_\pm = \frac{\hat{B}}{2\hat{A}} \pm \sqrt{\left(\frac{\hat{B}}{2\hat{A}} \right)^2 + \frac{\hat{C}}{\hat{A}}}, \quad (62)$$

with

$$\hat{A} = \frac{1}{2\hat{\kappa}^2 \hat{h}(r_+)}, \quad \hat{B} = \frac{\hat{h}'_\tau(r_+)}{\hat{\kappa} \hat{F}'(r_+)}, \quad \hat{C} = \frac{\hat{h}'(r_+)}{2\hat{h}(r_+)} \frac{1}{\hat{F}'(r_+)}. \quad (63)$$

The butterfly velocities \hat{v}_B^\pm for the ultraspinning Kerr-AdS black hole is shown in Figure 2. It can be seen that the negative modes \hat{v}_B^- are larger compared to the positive modes \hat{v}_B^+ although in this case, we do not observe any velocities that violate the speed of light. The butterfly velocities for the ultraspinning case also approach zero at extremality, similar to the standard Kerr-AdS black hole cases. As expected from the $\hat{r}_c(\mathcal{L})$ dependence on \mathcal{L} , the butterfly velocities are larger with larger value of \mathcal{L} . Furthermore, the butterfly velocity blows up in the extreme limit of $s = 1$ case due to the factor $(1 - \hat{\Omega}_\varphi \mathcal{L})^{-1}$ in the butterfly velocity.

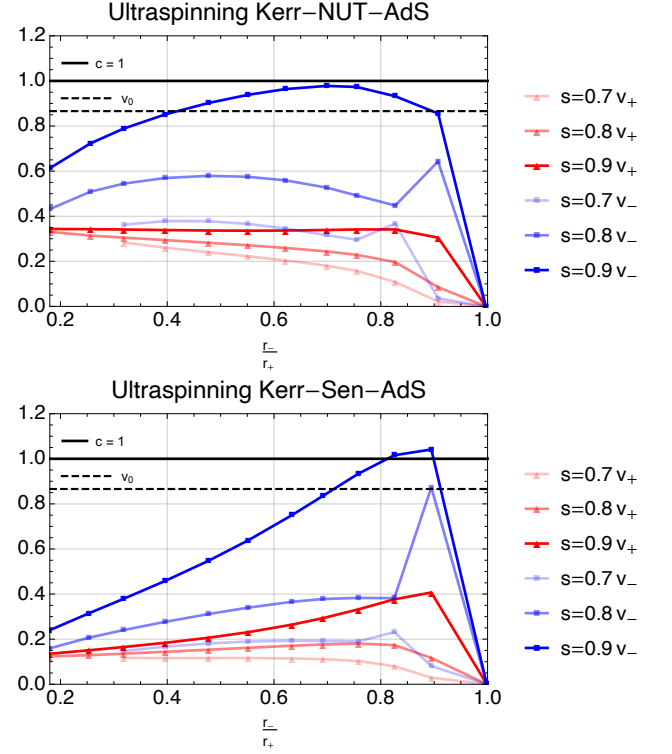


FIG. 2. Plot for the butterfly velocities \hat{v}_B^\pm of the ultraspinning Kerr-NUT-AdS (top) with $n = 0.05$ and Kerr-Sen-AdS (bottom) black hole. The angular momentum \mathcal{L} is again scaled as $\mathcal{L} = s\tau/\hat{\Omega}_\varphi$. We plot for $s = \{0.7, 0.8, 0.9\}$ from $s = 0.7$ which is depicted by the line with lowest opacity up to $s = 0.9$ which is the one with solid line. Blue lines represent \hat{v}_B^- while red lines represent \hat{v}_B^+ . In this case we use $p = 0.2, q = 0.1, l = 1$.

VI. LYAPUNOV EXPONENT

It has been shown recently [22] that a more general rotating black hole in AdS with extra conserved charges also exhibits chaos. Using the holographic calculation of the mutual information, the scrambling time can be obtained to have a logarithmic nature $\tau_* \sim \log S$ at the leading term or large entropy limit with $r_+/l \gg 1$. Furthermore, the minimum instantaneous Lyapunov exponent [19] can also be obtained from

$$\lambda_L = \frac{4\pi \sqrt{-F(r_*)h(r_*)}}{\mathcal{A}_H}, \quad (64)$$

where r_* is the solution to $\frac{d}{dr}(F(r)h(r))|_{r=r_*} = 0$ and \mathcal{A}_H is the area of the horizon.

In this section, we show how the minimum instantaneous Lyapunov exponent varies with respect to the ratio $\tau \equiv r_-/r_+$ ranging from 0 to 1 (extreme limit). We also plot the surface gravity analog κ and see whether the bound $\lambda_L \leq \kappa$ is still obeyed. We choose the black hole parameters such that the large entropy limit $r_+/l \gg 1$ can still be used. The result is shown in Figure 3 for the

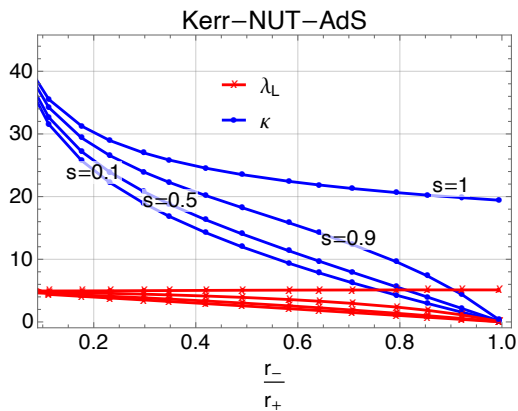


FIG. 3. Plot of both κ and λ_L with $\mathcal{L} = s\tau/\mu$ for the Kerr-NUT-AdS black hole. The parameters of the black hole are $a = 0.05, l = 0.1, p = 0.2, q = 0.1, n = 0.03$. The ratio $r_+/l > 1$ is also maintained. The range of the mass parameter is $m \in [1.5, 0.3994]$ and the range of the ratio r_+/l is $r_+/l \in [2.84701, 1.02866]$.

Kerr-NUT-AdS black hole and Figure 4 for the Kerr-Sen-AdS counterpart. In contrast with the Lyapunov plot in [22], in this work, we make sure that the value of r_+/l is always greater than one, although it becomes closer to one as we approach the extreme limit $\tau \rightarrow 1$.

It can be shown from the graph that the behavior of the Lyapunov exponent λ_L between the Kerr-Sen-AdS and Kerr-NUT-AdS black holes are quite different, especially for large values of \mathcal{L} . The value of $\mathcal{C} \equiv \kappa/\lambda_L$ are $\mathcal{C} = 7.7363$ for the Kerr-NUT-AdS black hole with $\tau = 0.582711$ and $\mathcal{C} = 1.53271$ for the Kerr-Sen-AdS black hole with $\tau = 0.55617$. We may conclude that the Kerr-Sen-AdS black hole is more chaotic than the Kerr-NUT-AdS black hole.

In the extremal limits, only the ones with $s = 1$ approach some finite non-zero values of λ_L while the other ones go to zero. This fact, along with the observation that the butterfly velocity also approaches zero in the extremal limit, shows that entanglement disruption cannot spread and will not scramble the TFD state in the extremal limit. However, the $s = 1$ case might not be physical in the extremal limit since in this case, both positive and negative modes of the butterfly velocity diverge.

VII. CONCLUSIONS AND DISCUSSIONS

The rotating and charged Kerr-AdS black hole families are chaotic under the perturbations with local rotating and charged shock waves. The local perturbations disrupt the entanglement pattern encoded in the TFD state and make the OTOC vanish inside the effective "light cone" created by both the scrambling time and the butterfly velocity. We show that aside from the logarithmic behavior of the scrambling time which indicates fast scrambling, the butterfly velocity can also be

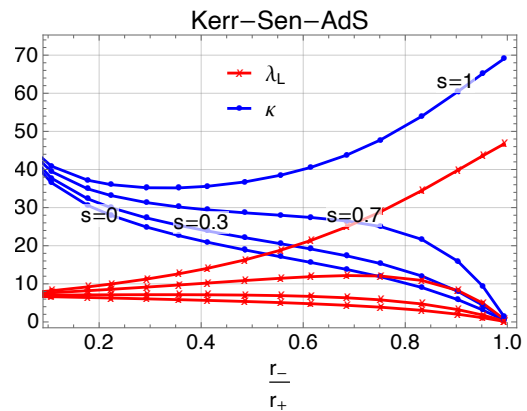


FIG. 4. Similar plot of both κ and λ_L with $\mathcal{L} = s\tau/\mu$ for the Kerr-Sen-AdS black hole. We choose $a = 0.05, l = 0.1, q = 0.2, p = 0.1$. We then vary the mass from $m = 1.5$ where $\tau \rightarrow 0$ to $m = 0.24905$ where we approach extremality. The ratio $r_+/l > 1$ is always maintained, ranging from $r_+/l = 2.91344$ to $r_+/l = 1.19766$.

obtained using holography. It is shown that there are two modes of the butterfly velocity; one which obeys the causality bound $c = 1$ as well as the Schwarzschild-AdS limit $v_{B0} = \sqrt{3}/2$ and the other one can exceed the speed of light and thus violating causality.

The result might indicate that there is only one mode of the butterfly velocity which is physical. This is unique to the rotating charged black hole case since the extra factor $\frac{B}{2A}$ breaks the symmetry between v_B^- and v_B^+ . This phenomenon was also observed in [14] for the three-dimensional BTZ black hole and it turns out that the four-dimensional Kerr-AdS black hole families are no exception. We may suspect that the superluminal behavior of one of the butterfly velocity modes also appears in other rotating AdS black holes such as the ones with higher curvature terms or even higher dimensional rotating black holes. This needs to be investigated further.

The holographic calculation of the butterfly velocity for the rotating charged Kerr-AdS black hole families in four dimensions is important to further study the properties of the dual CFT. By knowing the black hole calculation first, it may open valuable insights to the microscopic description of the dual three-dimensional CFT which is described earlier by the entangled TFD state with extra chemical potentials due to rotation and charges. The angular momentum \mathcal{L} and charges \mathcal{Q}, \mathcal{P} also play important roles in the chaotic properties of the black hole and hence also provide more insights to the microscopic CFT dual description.

The angular momentum of the shock waves \mathcal{L} increases both the butterfly velocity and the Lyapunov exponent. We also find that the butterfly velocity for all values of $s \neq 1$ approaches zero in the extremal limit, along with the Lyapunov exponent. From here, we can conclude that chaos might not happen in the extremal limit of Kerr-AdS black hole families. Moreover, although the

Lyapunov exponent reaches some non-zero value at extremality when $s = 1$, the butterfly velocity in this frame of reference diverges for both modes. This result will give us more insight into understanding chaos for extremal rotating and charged black holes and their dual theories.

The electric and magnetic charges of the shock waves \mathcal{Q}, \mathcal{P} defined in [22] do not have a direct influence on both butterfly velocities and the Lyapunov exponent (and even the scrambling time τ_*). However, the charges play a very important role in delaying the scrambling process of the black hole [47]. The charge of the shock waves interacts with the black hole charge, creating a "bounce" inside the black hole horizon so that the shock waves change their direction in the interior. The difference between the time of the bounce τ_d and the time when the shock waves are sent from the boundary τ_0 denotes the scrambling delay time and it is highly influenced by the shock wave charges. For the four-dimensional Kerr-AdS black hole families, the result is given by Eq. (109) of [22], which also applies to other various Kerr-AdS black hole families.

It is also interesting to study chaos for black holes other than AdS. However, this needs a different approach than the TFD state description of the entangled dual CFT. For

instance, as mentioned earlier, rotating black holes have some CFT description near extremality near its horizon via the Kerr/CFT [30–36]. Investigating chaos due to small perturbations in this framework may also be interesting, which is left for future works.

ACKNOWLEDGMENTS

F. P. Z. would like to thank Kemenristek, the Ministry of Research, Technology, and Higher Education, Republic of Indonesia for financial support. H. L. P. would like to thank Ganesha Talent Assistantship Institut Teknologi Bandung for financial support. H. L. P. would like to thank the members of the Theoretical Physics Groups of Institut Teknologi Bandung for their hospitality. D. D. is supported financially by Directorate of of Talent Management BRIN (Badan Riset dan Inovasi Nasional) for his postdoctoral fellowship. S. A. was supported by an appointment to the Young Scientist Training Program at the Asia Pacific Center for Theoretical Physics (APCTP) through the Science and Technology Promotion Fund and Lottery Fund of the Korean Government. This was also supported by the Korean Local Governments - Gyeongsangbuk-do Province and Pohang City.

-
- [1] S. H. Shenker and D. Stanford, Black holes and the butterfly effect, *Journal of High Energy Physics* **2014**, 10.1007/JHEP03(2014)067 (2014).
 - [2] J. Maldacena, S. H. Shenker, and D. Stanford, A bound on chaos, *Journal of High Energy Physics* **2016**, 10.1007/JHEP08(2016)106 (2016).
 - [3] J. Maldacena, The Large N Limit of Superconformal Field Theories and Supergravity, *Int. J. Theor. Phys.* **38**, 1113 (1999).
 - [4] S. Ryu and T. Takayanagi, Holographic Derivation of Entanglement Entropy from the anti-de Sitter Space/Conformal Field Theory Correspondence, *Phys. Rev. Lett.* **96**, 181602 (2006).
 - [5] S. Ryu and T. Takayanagi, Aspects of holographic entanglement entropy, *J. High Energ. Phys.* **08**, 45.
 - [6] V. E. Hubeny, M. Rangamani, and T. Takayanagi, A covariant holographic entanglement entropy proposal, *J. High Energ. Phys.* **2007** (07), 62.
 - [7] T. Hartman and J. Maldacena, Time evolution of entanglement entropy from black hole interiors, *Journal of High Energy Physics* **2013**, 10.1007/JHEP05(2013)014 (2013).
 - [8] S. Leichenauer, Disrupting entanglement of black holes, *Physical Review D - Particles, Fields, Gravitation and Cosmology* **90**, 10.1103/PhysRevD.90.046009 (2014).
 - [9] D. A. Roberts, D. Stanford, and L. Susskind, Localized shocks, *Journal of High Energy Physics* **2015**, 10.1007/JHEP03(2015)051 (2015).
 - [10] V. Jahnke, Delocalizing entanglement of anisotropic black branes, *Journal of High Energy Physics* **2018**, 10.1007/JHEP01(2018)102 (2018).
 - [11] D. Ávila, V. Jahnke, and L. Patiño, Chaos, diffusivity, and spreading of entanglement in magnetic branes, and the strengthening of the internal interaction, *Journal of High Energy Physics* **2018**, 10.1007/JHEP09(2018)131 (2018).
 - [12] W. Fischler, V. Jahnke, and J. F. Pedraza, Chaos and entanglement spreading in a non-commutative gauge theory, *Journal of High Energy Physics* **2018**, 10.1007/JHEP11(2018)072 (2018).
 - [13] Y. Ahn, V. Jahnke, H. S. Jeong, and K. Y. Kim, Scrambling in hyperbolic black holes: shock waves and pole-skipping, *Journal of High Energy Physics* **2019**, 10.1007/JHEP10(2019)257 (2019).
 - [14] V. Jahnke, K. Y. Kim, and J. Yoon, On the chaos bound in rotating black holes, *Journal of High Energy Physics* **2019**, 10.1007/JHEP05(2019)037 (2019).
 - [15] R. R. Poojary, BTZ dynamics and chaos, *Journal of High Energy Physics* **2020**, 10.1007/JHEP03(2020)048 (2020).
 - [16] A. Banerjee, A. Kundu, and R. R. Poojary, Rotating black holes in AdS spacetime, extremality, and chaos, *Physical Review D* **102**, 10.1103/PhysRevD.102.106013 (2020).
 - [17] M. Blake and R. A. Davison, Chaos and pole-skipping in rotating black holes, *Journal of High Energy Physics* **2022**, 10.1007/JHEP01(2022)013 (2022).
 - [18] V. Malvimat and R. R. Poojary, Fast scrambling due to rotating shockwaves in BTZ, *Physical Review D* **105**, 10.1103/PhysRevD.105.126019 (2022).
 - [19] V. Malvimat and R. R. Poojary, Fast scrambling of mutual information in Kerr-AdS4 spacetime, *Physical Review D* **107**, 10.1103/PhysRevD.107.026019 (2023).

- [20] V. Malvimat and R. R. Poojary, Fast scrambling of mutual information in Kerr-AdS5, *Journal of High Energy Physics* **2023**, 10.1007/jhep03(2023)099 (2023).
- [21] M. A. Amano, M. Blake, C. Cartwright, M. Kaminski, and A. P. Thompson, Chaos and pole-skipping in a simply spinning plasma, *Journal of High Energy Physics* **2023**, 10.1007/JHEP02(2023)253 (2023).
- [22] H. L. Prihadi, F. P. Zen, D. Dwiputra, and S. Ariwahjoedi, Chaos and fast scrambling delays of a dyonic kerr-sen-ads₄ black hole and its ultraspinning version, *Phys. Rev. D* **107**, 124053 (2023).
- [23] Q. Q. Zhao, Y. Z. Li, and H. Lü, Static equilibria of charged particles around charged black holes: Chaos bound and its violations, *Physical Review D* **98**, 10.1103/PhysRevD.98.124001 (2018).
- [24] B. Gwak, N. Kan, B. H. Lee, and H. Lee, Violation of bound on chaos for charged probe in Kerr-Newman-AdS black hole, *Journal of High Energy Physics* **2022**, 10.1007/JHEP09(2022)026 (2022).
- [25] C. Yu, D. Chen, and C. Gao, Bound on Lyapunov exponent in Einstein-Maxwell-Dilaton-Axion black holes, *Chinese Physics C* **46**, 10.1088/1674-1137/ac90af (2022).
- [26] C. Yu, D. Chen, B. Mu, and Y. He, Violating the chaos bound in five-dimensional, charged, rotating Einstein-Maxwell-Chern-Simons black holes, *Nuclear Physics B* **987**, 10.1016/j.nuclphysb.2023.116093 (2023).
- [27] Y. He, Z. Wang, and D. Chen, Report on chaos bound outside taub-nut black holes, *Physics of the Dark Universe* **42**, 101325 (2023).
- [28] D. Chen and C. Gao, Chaos bound in Kerr-Newman-Taub-NUT black holes via circular motions*, *Chinese Physics C* **47**, 10.1088/1674-1137/ac9fb9 (2023).
- [29] J. Maldacena, Eternal black holes in anti-de Sitter, *J. High Energ. Phys.* **04**, 21.
- [30] M. Guica, T. Hartman, W. Song, and A. Strominger, The Kerr/CFT correspondence, *Physical Review D - Particles, Fields, Gravitation and Cosmology* **80**, 1 (2009), arXiv:0809.4266.
- [31] M. F. Sakti, A. Suroso, and F. P. Zen, CFT duals on extremal rotating NUT black holes, *International Journal of Modern Physics D* **27**, 10.1142/S0218271818501092 (2018).
- [32] M. F. Sakti, A. Suroso, and F. P. Zen, Kerr/CFT correspondence on Kerr-Newman-NUT-Quintessence black hole, *European Physical Journal Plus* **134**, 10.1140/epjp/i2019-12937-x (2019).
- [33] M. F. Sakti, A. Suroso, and F. P. Zen, Kerr-Newman-NUT-Kiselev black holes in Rastall theory of gravity and Kerr/CFT correspondence, *Annals of Physics* **413**, 10.1016/j.aop.2019.168062 (2020), arXiv:1901.09163.
- [34] M. F. Sakti, A. M. Ghezelbash, A. Suroso, and F. P. Zen, Hidden conformal symmetry for Kerr-Newman-NUT-AdS black holes, *Nuclear Physics B* **953**, 10.1016/j.nuclphysb.2020.114970 (2020).
- [35] M. F. Sakti and F. P. Zen, CFT duals on rotating charged black holes surrounded by quintessence, *Physics of the Dark Universe* **31**, 10.1016/j.dark.2021.100778 (2021).
- [36] M. F. Sakti and P. Burikham, Dual CFT on a dyonic Kerr-Sen black hole and its gauged and ultraspinning counterparts, *Physical Review D* **106**, 10.1103/PhysRevD.106.106006 (2022).
- [37] Y. Sekino and L. Susskind, Fast scramblers, *Journal of High Energy Physics* **2008**, 10.1088/1126-6708/2008/10/065 (2008).
- [38] C. Rovelli and L. Smolin, Loop space representation of quantum general relativity, *Nuclear Physics, Section B* **331**, 10.1016/0550-3213(90)90019-A (1990).
- [39] S. Ariwahjoedi, J. S. Kosasih, C. Rovelli, and F. P. Zen, How many quanta are there in a quantum space-time?, *Classical and Quantum Gravity* **32**, 10.1088/0264-9381/32/16/165019 (2015).
- [40] The electrically and magnetically charged Kerr-NUT-AdS black hole is called the Kerr-Newman-NUT-AdS black hole. However, in this work, we refer the Kerr-NUT-AdS to the charged version as well for brevity.
- [41] J. B. Griffiths and J. Podolský, A new look at the Plebański-Demiański family of solutions, *International Journal of Modern Physics D* **15**, 10.1142/S0218271806007742 (2006).
- [42] N. H. Rodríguez and M. J. Rodríguez, First law for Kerr Taub-NUT AdS black holes, *Journal of High Energy Physics* **2022**, 10.1007/JHEP10(2022)044 (2022).
- [43] D. Wu, S. Q. Wu, P. Wu, and H. Yu, Aspects of the dyonic Kerr-Sen-AdS₄ black hole and its ultraspinning version, *Physical Review D* **103**, 10.1103/PhysRevD.103.044014 (2021).
- [44] T. Dray and G. 't Hooft, The effect of spherical shells of matter on the Schwarzschild black hole, *Communications in Mathematical Physics* **99**, 10.1007/BF01215912 (1985).
- [45] T. Dray and G. 't Hooft, The gravitational shock wave of a massless particle, *Nuclear Physics, Section B* **253**, 10.1016/0550-3213(85)90525-5 (1985).
- [46] M. Mezei and G. Sárosi, Chaos in the butterfly cone, *Journal of High Energy Physics* **2020**, 10.1007/JHEP01(2020)186 (2020).
- [47] G. T. Horowitz, H. Leung, L. Queimada, and Y. Zhao, Bouncing inside the horizon and scrambling delays, *Journal of High Energy Physics* **2022**, 10.1007/JHEP11(2022)025 (2022).